CHALMERS

Chalmers Publication Library

(article starts on next page)

Optical sectioning for measurements in transient sprays

Mattias Rahm,[1,*] **Zachary Falgout,**[1] **David Sedarsky,**[1] **and Mark Linne**[2]

[1]*Applied Mechanics, Chalmers University of Technology, SE-41296, Gothenburg, Sweden*
[2]*School of Engineering, University of Edinburgh, Mayfield Road, Edinburgh, EH9 3DW, UK*
[*]*mattias.rahm@chalmers.se*

Abstract: We describe a practical arrangement for optical sectioning by means of time-gated backscatter imaging using ultrafast illumination and a CS_2-based optical Kerr effect shutter. This arrangement can reveal additional information when probing transient turbid media such as fuel injection sprays or complex multiphase flows which require single-shot imaging with sufficient time resolution to freeze the dynamics of the flow.

References and links

1. M. Linne, "Imaging in the optically dense regions of a spray: A review of developing techniques," Prog. Energy Combust. Sci. **39**, 403–440 (2013).
2. L. Wang, P. P. Ho, C. Liu, G. Zhang, and R. R. Alfano, "Ballistic 2-d imaging through scattering walls using an ultrafast optical kerr gate," Science **253**, 769–771 (1991).
3. L. Wang, P. P. Ho, X. Liang, H. Dai, and R. R. Alfano, "Kerr-fourier imaging of hidden objects in thick turbid media," Opt. Lett. **18**, 241–243 (1993).
4. M. Paciaroni and M. Linne, "Single-shot, two-dimensional ballistic imaging through scattering media," Appl. Opt. **43**, 5100–5109 (2004).
5. M. Linne, M. Paciaroni, T. Hall, and T. Parker, "Ballistic imaging of the near field in a diesel spray," Exp. Fluids **40**, 836–846 (2006).
6. M. Linne, M. Paciaroni, J. Gord, and T. Meyer, "Ballistic imaging of the liquid core for a steady jet in crossflow," Appl. Opt. **44**, 6627–6634 (2005).
7. M. Paciaroni, M. Linne, T. Hall, J. P. Delplanque, and T. Parker, "Single-shot two-dimensional ballistic imaging of the liquid core in an atomizing spray," Atomization Spray **16**, 51–69 (2006).
8. D. Sedarsky, J. Gord, C. Carter, T. Meyer, and M. Linne, "Fast-framing ballistic imaging of velocity in an aerated spray," Opt. Lett. **34**, 2748–2750 (2009).
9. J. B. Schmidt, Z. D. Schaefer, T. R. Meyer, S. Roy, S. A. Danczyk, and J. R. Gord, "Ultrafast time-gated ballistic-photon imaging and shadowgraphy in optically dense rocket sprays," Appl. Opt. **48**, B137–B144 (2009).
10. Z. Falgout, M. Rahm, D. Sedarsky, and M. Linne, "Gas/fuel jet interfaces under high pressures and temperatures," Fuel **168**, 14–21 (2016).
11. S. Idlahcen, L. Mees, C. Roze, T. Girasole, and J. B. Blaisot, "Time gate, optical layout, and wavelength effects on ballistic imaging," J. Opt. Soc. Am. A **26**, 1995–2004 (2009).
12. D. Sedarsky, E. Berrocal, and M. Linne, "Quantitative image contrast enhancement in time-gated transillumination of scattering media," Opt. Express **19**, 1866–1883 (2011).
13. S. Idlahcen, C. Roze, L. Mees, T. Girasole, and J.-B. Blaisot, "Sub-picosecond ballistic imaging of a liquid jet," Exp. Fluids **52**, 289–298 (2012).
14. H. Purwar, S. Idlahcen, C. Roze, D. Sedarsky, and J.-B. Blaisot, "Collinear, two-color optical kerr effect shutter for ultrafast time-resolved imaging," Opt. Express **22**, 15778–15790 (2014).
15. M. Rahm, M. Paciaroni, Z. Wang, D. Sedarsky, and M. Linne, "Evaluation of optical arrangements for ballistic imaging in sprays," Opt. Express **23**, 22444–22462 (2015).
16. E. Kristensson, E. Berrocal, M. Richter, S.-G. Pettersson, and M. Alden, "High-speed structured planar laser illumination for contrast improvement of two-phase flow images," Opt. Lett. **33**, 2752–2754 (2008).

17. E. Berrocal, E. Kristensson, P. Hottenbach, M. Alden, and G. Grunefeld, "Quantitative imaging of a non-combusting diesel spray using structured laser illumination planar imaging," Appl. Phys. B **109**, 683–694 (2012).
18. E. Kristensson, L. Araneo, E. Berrocal, J. Manin, M. Richter, M. Alden, and M. Linne, "Analysis of multiple scattering suppression using structured laser illumination planar imaging in scattering and fluorescing media," Opt. Express **19**, 13647–13663 (2011).
19. A. G. Podoleanu, "Optical coherence tomography," J. Microsc. **247**, 209–219 (2012).
20. S. Demos, H. Radousky, and R. Alfano, "Deep subsurface imaging in tissues using spectral and polarization filtering," Opt. Express **7**, 23–28 (2000).
21. S. A. Kartazayeva, X. Ni, and R. R. Alfano, "Backscattering target detection in a turbid medium by use of circularly and linearly polarized light," Opt. Lett. **30**, 1168–1170 (2005).
22. M. E. Zevallos L., S. K. Gayen, M. Alrubaiee, and R. R. Alfano, "Time-gated backscattered ballistic light imaging of objects in turbid water," Appl. Phys. Lett. **86**, 011115 (2005).
23. R. N. Dahms, J. Manin, L. M. Pickett, and J. C. Oefelein, "Understanding high-pressure gas-liquid interface phenomena in diesel engines," P. Combust. Inst. **34**, 1667–1675 (2013).
24. C. Baumgarten, *Mixture Formation in Internal Combustion Engines* (Springer, 2006).

1. Introduction

Imaging transient phenomena presents a particular challenge for optical diagnostics when applied to fluid mechanical problems. Here both temporal and spatial resolution are important. For most imaging scenarios this entails single-shot measurements of the full field-of-view (FOV) with exposure times short enough to suppress detectable motion in the imaged field (on the order of 1–10 μs). Turbid transient media, such as atomizing sprays, also suffer from attenuation and multiple-scattering interference. This presents a further imaging difficulty. The high optical depths (OD) present in important regions of atomizing sprays limit the dynamic range of detectable optical signals and they limit the capacity to acquire an image unless scattered-light mitigation strategies are employed to filter the collected image signal.

Ballistic Imaging (BI) is a technique that exploits schemes to suppress significant image corruption caused by multiple light scattering off-axis from the dense cloud of droplets present in the spray formation region [1]. This image corruption limits the applicability of more conventional imaging approaches when studying highly atomizing fuel sprays used in modern direct injection combustion engines. BI was originally developed to address imaging through human tissue, and the time-gated approach, based on the Optical Kerr Effect (OKE), was introduced by the group of Alfano at the City University of New York (see e.g. [2, 3]). The time-gated technique relies on ultra-short laser pulses ($\sim$ 100 fs) and an OKE activated shutter along the optic axis to suppress the influence of multiply scattered off-axis light (corrupted light) based on its time-of-flight. In a transillumination arrangement, multiply scattered off-axis light containing severely corrupted image information exits the scattering medium later than the higher quality imaging light. Using an OKE-gate that is timed to emphasize high quality image light suppresses the contribution from the corrupted light. Since BI is performed in a transillumination arrangement, it can provide line-of-sight information on the liquid/gas interfaces inside the scattering drop cloud that surrounds the spray formation region. The first application of BI to sprays relevant to direct injection internal combustion engines was reported by Paciaroni and Linne in the mid-2000s [4, 5]. Since then a number of different sprays have been studied, *e.g.* [6–10]. Given its applicability to such sprays, further development of the technique is an active area of research [11–15].

Another approach is to detect the side- and backscattered light from within scattering media. Structured laser illumination planar imaging (SLIPI) is a technique that has successfully been applied to detect singly side scattered light in moderately dense sprays [16]. It has for example been applied to a Diesel spray under non-combusting conditions as a way to reduce multiple scattering errors when using planar droplet sizing (PDS) [17]. Kristensson *et al.* assessed SLIPI to be functional up to an OD $\sim$6 [18]. The technique can thus run into difficulties when probing

the spray formation region of highly atomizing sprays.

Detection of backscattered light is done in *e.g.* medical Optical Coherence Tomography (OCT) and Spectral Polarization Difference Imaging (SPDI) [19–21]. In OCT singly backscattered, coherent light from a white light beam which is focused inside tissue is detected using interference from a reference beam. Multiply scattered light will have progressively degraded coherence, and will therefore not contribute to the interference. In OCT the image is formed by raster scanning the sample either in a transverse plane and/or in depth. Such techniques are probably not applicable to sprays because, as discussed in reference [1], to image a spray requires capturing an entire image within several microseconds. There are an insufficient number of coherent photons exiting a genuinely dense spray to construct an entire image within the required time frame. In SPDI and related techniques, polarization characteristics of the backscattered light are used to suppress unwanted contributions to the image. Incident light with a well-defined polarization state illuminates the sample and the backscattered image is filtered with additional polarizers. Backscattering from the sample surface will predominantly maintain the polarization state of the illuminating light while multiple light scattering from within the sample will have lost its initial polarization. In this way, contributions from surface and sub-surface scattering can be differentiated. By generating and combining images using different illumination wavelengths, the wavelength dependent penetration-depth can be used to accentuate depth within the sample.

In 2005 Zevallos *et al.* investigated the use of a time-gate to suppress multiple scattering noise in a backscattered image [22]. They used both 130 fs and 3.5 ns laser pulses centered on 800 nm with an average beam power of 60 mW. For a time-gate they used a fast-gated intensified camera system capable of generating shutter-times between 80 ps and 6 ns. They investigated the backscattered signal from a test chart placed in the center of a 100x100x50 mm^3 cuvette filled with 0.5 μm TiO$_2$ particles suspended in distilled water. Their results showed that the short-pulse/short-gate combination (130 fs/80 ps) was the only combination capable of generating a visible backscattering image of the test chart.

In this article we investigate the use of a short-pulse, time-gated backscattering setup intended to provide information in the spray formation region of atomizing sprays. Here the time-gated ballistic imaging technique previously used in transillumination arrangements is modified to form a backscattering optical system. Using a single color crossed-beam OKE gating geometry, gate-times around 1.5 ps can be achieved using carbon disulfide (CS$_2$) as the Kerr medium. Similar to ballistic imaging, unwanted light contributions can be suppressed based on both their polarization and temporal characteristics. Ultimately this technique has the potential to extract a scattered signal from a well-defined planar section of the scattering medium, *i.e.* a form of optical sectioning within the object.

2. Experiments

The experiments were performed in the high-pressure, high temperature spray research chamber at Chalmers University. This vessel operates with a steady flow of heated, pressurized air moving downwards through the chamber. The vessel can maintain steady conditions of up to 90 bar with temperatures up to 1000 K. Temperature is maintained by continuous injection of electrically heated air into the chamber. The air flow is slow relative the dynamics of the fuel spray, but it provides sufficient flow for steady operation over the full temperature and pressure range. Bidirectional optical access is provided along orthogonal axes through the center of the chamber by two pairs of vertically oriented oval windows. The fuel injector was a single-hole, plain orifice Bosch model CRIP-2 (diameter= 140 μm, P$_{inj}$=150 MPa). The fuel was delivered using a 3-stage reciprocating piston pump (identical to pumps used on commercial truck engines) and single injections on the order of 1.8 ms were used. The spray images were all

captured during the steady period of the injection.

An optical schematic is shown in Fig. 1. The light source consists of a mode-locked Ti:sapphire oscillator (Spectra-Physics Mai Tai) generating ~80 fs pulses at 82 MHz repetition rate with an average power around 1.5 W. The oscillator seeds a chirped-pulse regenerative amplifier (Spectra-Physics Spitfire) which emits amplified pulses at 1 kHz. The pulses are on the order of 100 fs FWHM centered on 800 nm with pulse energies of 4 mJ and a beam diameter of 8 mm ($1/e^2$). The beam from the amplifier was split with a 50.8 mm diameter 50% beam-splitter into an image beam illuminating the spray and a gating beam activating the OKE-gate.

The image beam illuminated the spray through one of the windows on the spray chamber. The backscattered light was collected and the image generated with a single 50.8 mm diameter, 150 mm focal length, AR-coated achromatic doublet in a $2f$-arrangement [15]. The angle between the image beam and the optical axis of the imaging system was around 25°. After the collecting lens, the image signal was split into a time-gated (TG) and a non-time-gated (non-TG) image signal with an additional beamsplitter. In this way simultaneous TG and non-TG versions of the backscattering image could be generated and collected by matched cameras. The non-TG part was directed to its camera with a turning mirror. The TG part was passed through the OKE-gate consisting of a Kerr medium surrounded by two crossed Glan-Laser Calcite polarizers with clear apertures of 15x15 mm^2. The cell containing the Kerr medium (CS_2) had a 40 mm aperture with a 10 mm path length. The images (TG and non-TG) were captured with two intensified CCD cameras (Princeton Instruments PI-MAX4 ICCD).

The gate beam was directed through a time delay (TD) to control the temporal overlap of the image pulse and the gate pulse. The TD was placed on a μm-translation stage to accurately control adjustments in optical path length (OPL) of the gate beam. The angle between the gate beam and the image beam in the Kerr cell was around 18°. By activating the CS_2 with a pulse from the gating beam, a time-gate acting along the imaging axis on the order of 1.5 ps could be generated. Both the imaging and gate beams used pulse energies of 0.35 mJ. The resulting OKE-gate efficiency was around 60%.
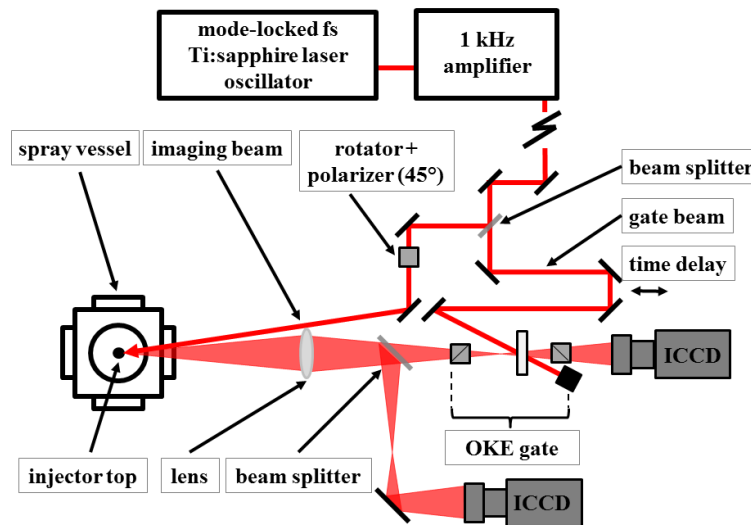

Fig. 1. Experimental setup. The initial beam is separated into an imaging beam and a gating beam controlling the OKE-gate. The backscattered signal is split into a TG part and a non-TG part and directed to the cameras.

Initially a ground glass tube was used as a backscatter-generating object to align the setup

and demonstrate successful time-gating in this new geometry. Once the setup was operational, both commercially available multi-component Diesel fuel and pure n-dodecane (henceforth referred to as dodecane) were injected into the chamber under two different conditions: 6 bar back-pressure at 293 K, and 60 bar back-pressure at 900 K. Throughout this article these two conditions will be referred to as low pressure-low temperature (LP-LT) and high pressure-high temperature (HP-HT) respectively. Note that the LP-LT condition is identical to the "Case 1" condition described by Falgout *et al.* [10], and it is very close to the lower pressure and temperature condition presented by Dahms *et al.* [23]. The HP-HT condition is very close to the "Spray A" condition discussed in Dahms *et al.* and it is identical to "Case 3" in Falgout *et al.* The articles by Dahms *et al.* and by Falgout *et al.* are concerned with the question of whether or not fuel jets become transitionally supercritical once the gas conditions reach the HP-HT condition.

3. Results and discussion

3.1. *Glass tube*

To investigate the viability of the time-gated backscattering approach initial experiments were performed on a ground glass tube placed immediately below the injector nozzle in the spray chamber. The ground glass tube had inner and outer diameters of 5.5 mm and 7 mm respectively. The tube and the injector tip are shown inside the chamber in Fig. 2. This photo of the tube was taken at 90° to the illumination direction.

The TD was used to scan the OKE-gate through the entire backscatter image, moving in steps of 0.05 mm (corresponding to 0.3 ps steps in time) and starting with the gate pulse ahead in time relative the image pulse. This time difference is related to the total path length travelled by the imaging light after the beamsplitter that separates the incoming beam into imaging- and gating components. That is, the time delay sets the path length of the light propagating to the scattering event and back through the OKE-gate, the "round-trip". A more intuitive measure is the time for the light to propagate from the scattering event to the OKE-gate, *i.e.* the "single-trip" time. This time, which can be approximated by halving the round-trip time, can readily be converted to distances in the region that has been probed, and is henceforth used when discussing TG-scans and corresponding distances within the object.
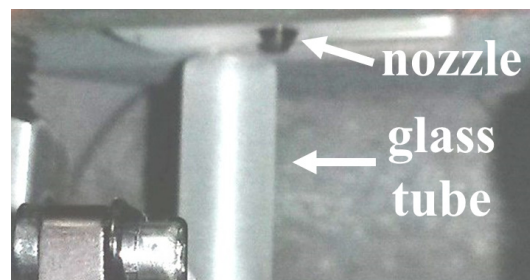

Fig. 2. Photo of the ground glass tube in place inside the spray chamber. The position of the injector tip is indicated in the image. The photo of the tube was taken at 90° to the illumination direction.

The TG-scan of the glass tube is shown in Fig. 3 (a video of the TG-scan is linked to it). The image depicts laser speckle from a roughened surface that is expanding in the horizontal direction owing to the curvature of the tube surface. Figure 4 presents the corresponding image mean intensities based on the recorded images as a function of the TD position. The signal maximum, which is centered on zero on the distance axis, corresponds to scattering from the

outer surface of the front face of the tube. Two secondary peaks are located 0.9 mm and 6.6 mm behind the primary peak respectively. Taking the curvature of the surfaces into account, the locations of the secondary peaks correspond to the measured dimensions of the glass tube. The first secondary peak (0.9 mm) arises from the inner surface of the front face, and the second secondary peak (6.6 mm) arises from the inner surface of the back face of the glass tube. A backscattering signal from the outer surface of the back face could not be distinguished above the background noise. Note also that the curves in Fig. 4 fairly closely follow the convolution of the OKE gate time (1.5 ps) with delta functions (interfaces).
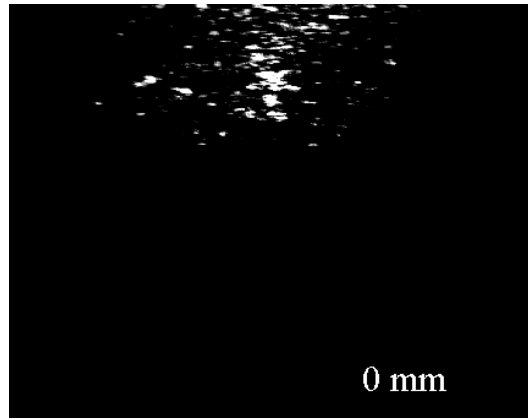

Fig. 3. Single-frame excerpt from TG-scan video of TG backscattering from glass tube (Visualization 1). Distances calculated from the "single-trip" time scale with zero centered on maximum intensity peak.
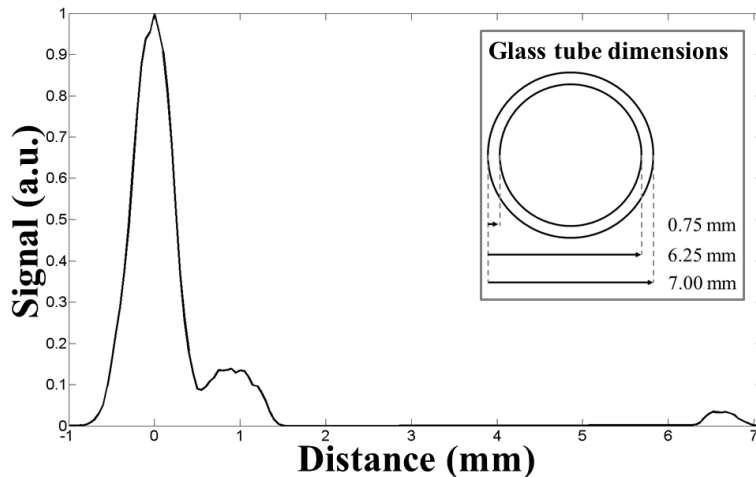

Fig. 4. Detected backscattering signal from a ground glass tube with the time-of-flight data converted to "single-trip" distances.

The experiments on the ground glass tube show that using the 1.5 ps OKE-gate enables separation of contributions to the total backscattering signal based on their temporal characteristics, and thus on their spatial position along the optic axis within the probed object. A TG of 1.5 ps corresponds to a light propagation distance of around 0.45 mm, meaning the depth resolution

along the optic axis is 0.45 mm with this gate length.

3.2. Fuel sprays

The optical setup was further applied to fuel sprays of Diesel and dodecane. These sprays were investigated under the two conditions described earlier; the LP-LT and the HP-HT conditions. In these experiments the TG was scanned through the backscattered signal starting with the gating pulse ahead of the image pulse in time and moving the TD in steps of 0.1 mm. This distance corresponds to 0.6 ps in the "round-trip" time, and 0.3 ps in the "single-trip" time. In each TD position, non-TG and TG images of ten separate spray events were recorded.

The images contain glare spots, which are unavoidable when detecting backscattered light from transparent liquid structures and droplets. As a consequence, the technique cannot reliably be used for drop sizing. As discussed by Falgout *et al.* in [10], however, BI investigations of the spray formation region of fuel sprays include evidence for a liquid core that grows in the downstream direction. This kind of structure could, for example, indicate a liquid core consisting of liquid sheets ("pancake structures", see *e.g.* Fig. 2.6 in [24]) with entrained gas between them. Indeed, BI, which is a line-of-sight technique, reveals liquid edges buried in scattering media. It cannot distinguish such depth-wise overlapping refractive structures. Therefore, other means of probing inside this style of core region must be employed. Time-gated backscattering has the potential to provide depth-resolved, qualitative information about structures, despite the presence of glare spots.

Figure 5 presents representative images of the non-TG and TG images in the LP-LT Diesel case. In the movie linked to Fig. 5, representative images from each TD step in the Diesel LP-LT are grouped together to generate a TG-scan of the signal. As can be seen in Fig. 5, high intensity structures are visible near the nozzle. A few of these structures, which most likely come from reflections from larger fluid structures in the spray formation region, have higher visibility in the TG image than in the non-TG version. This happens because the OKE-gate selects light propagating along a specific path length while suppressing contributions from the remaining part of the light signal; multiply scattered light as well as reflected light. Schematically speaking, this time filter transmits light emanating from scattering/reflection events within a planar probe-region of around 0.45 mm depth centered on the distance where the path length of the light overlaps with OKE-gate maximum transmittance.

In Fig. 6, representative non-TG and TG images of the HP-HT Diesel case are shown. These are the gas phase conditions that have been speculated to produce a diffusive mixing layer at the edge of the liquid core in a dodecane spray, rather than a well-defined liquid/gas interface [23]. In the movie linked to Fig. 6, representative images from each TD step are grouped together to generate a TG-scan of the signal. A trend in the HP-HT scan (both TG and non-TG) is that larger refractive liquid structures near the nozzle are seen less frequently. Furthermore, the spray images in the scan tend to move relative to the fixed position of the nozzle outline. This is in part an effect of refractive index gradients in the gas phase that surround the spray, they refract light as it propagates across the chamber and affect the apparent spray position. This can, for example, be seen near the nozzle and outside of the spray region where the non-TG images contain these refractive structures from the gas phase. Figure 7 contains the image from Fig. 6 but with adjusted contrast to make the gas phase refractive structures more visible. Because the time-gate samples light propagating along a specific path from a specific depth and not the complete image signal, these image effects are reduced in the TG image. Under the HP-HT conditions, the TG and non-TG dodecane spray images were very similar to the corresponding Diesel ones and will therefore not be included.

In Fig. 6 one can also see periodically clustered structures in the spray. This flow case was also discussed in Falgout *et al.* [10] (*i.e.* a Diesel fuel jet at the same pressure and temperature),
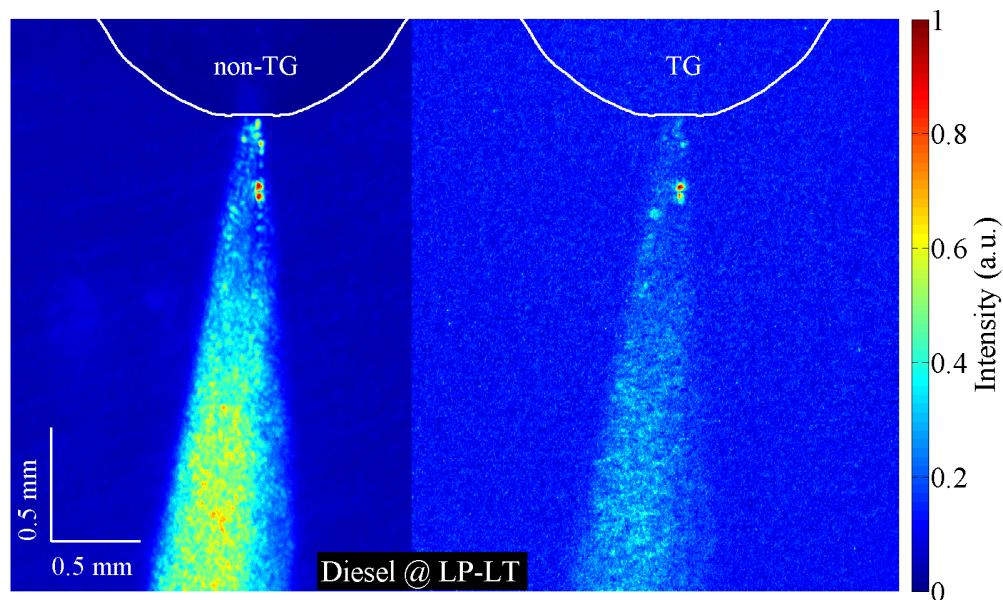
Fig. 5. TG and non-TG image of Diesel LP-LT shown in false color. The intensity has been normalized between 0 and 1 in each image. In the images a nozzle-tip outline has been added to help interpretation. Reflections from larger fluid structures near the nozzle have higher visibility in the TG case than in the non-TG case due to suppression of multiple scattering from the drop cloud surrounding the spray. A complete TG-scan from the Diesel LP-LT is provided as a video in Visualization 2.

in which it appeared that this fuel does not produce a diffusive mixing layer. Rather, all BI indications were that a liquid core structure with defined liquid/gas interfaces was maintained. In such a case one would hope to see additional structural details inside the spray using optical sectioning. At this point, however, one cannot state with certainty that the periodically clustered features in the TG image of Fig. 6 are indeed larger liquid features. The image light level was low, making image resolution difficult, but that can be improved in the future. There is also some evidence for glare spots emanating from a distributed surface, but higher signal levels are required to identify these image structures. Higher imaging power is a possibility, and it would help to magnify the area in question as well.

In Fig. 8, representative non-TG and TG images of the LP-LT dodecane case are shown, and a video is linked to the images as before. A trend for the dodecane sprays is that reflections from larger liquid structures near the nozzle are absent, even at the LP-LT conditions. One possible explanation would be that dodecane has a significantly lower viscosity than Diesel fuel, and this could lead to much more enhanced turbulent mixing in the liquid core and deposition of higher levels of kinetic energy into drop formation in the dodecane case. The surface tension of dodecane is also a bit lower, making it possible to generate smaller drop and ligament structures. In short, the physical properties of dodecane may preclude formation of the bigger structures observed in the Diesel jet.

Based on the ten images in each TD step in the TG-scans, mean signal intensities and standard deviations can be calculated. The results are shown in Figs. 9(a)–9(b). Figure 9(a) shows the Diesel case and Fig. 9(b) shows the dodecane case. Starting with the signals in the non-TG case; for both fuels the signal is noisier in the HP-HT condition than in the LP-LT condition. In the Diesel case the signal strength increased when going up in pressure and temperature. In the
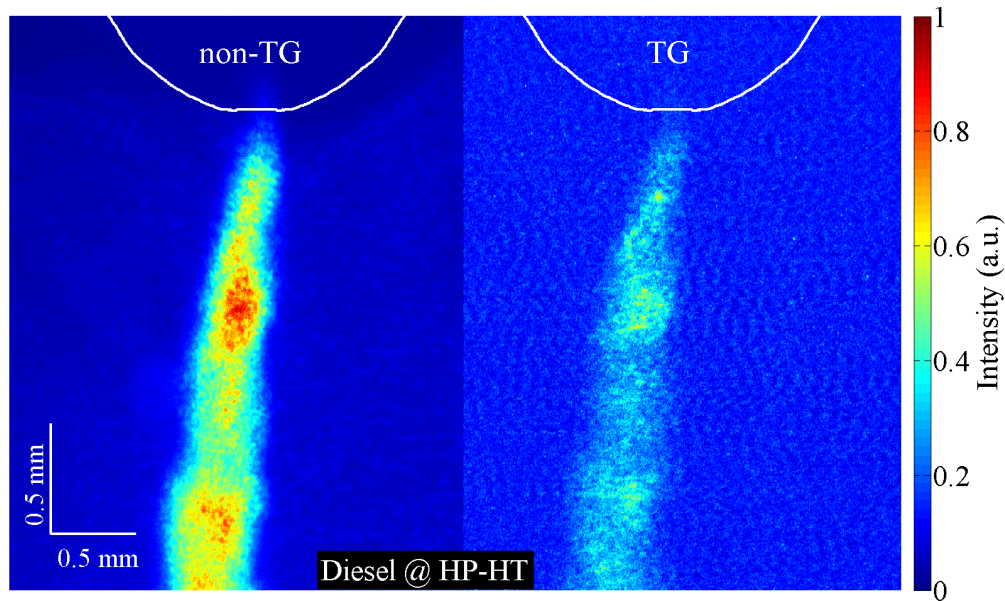
Fig. 6. TG and non-TG image of Diesel HP-HT shown in false color. The intensity has been normalized between 0 and 1 in each image. In the images a nozzle-tip outline has been added to help interpretation. Larger refractive liquid structures near the nozzle are seen less frequently in the Diesel HP-HT case than in the Diesel LP-LT case. A complete TG-scan from the Diesel HP-HT is provided as a video in Visualization 3.

dodecane case, on the other hand, the opposite is true. Here the strength of the non-TG signal decreased when going up in pressure and temperature. These differences are likely caused by differences in physical properties again. The HP-HT case is well above the boiling point of dodecane but it is closer to the boiling points of some heavier ends in the Diesel fuel. As temperature and pressure climb, the dodecane jet probably becomes optically thin as the smaller drops vaporize quickly. In the Diesel case it is likely that the spray breaks up even more vigorously than at the LP-LT condition, contributing to higher scattering light levels and stronger variations.

The TG-scans are similar in all cases. The signals include a temporal profile with a FWHM around 7 ps. It should be noted that the temporal dependence of the scattering signal depends both on the spatial dimensions of the spray, the size distribution and concentration of the scattering drops, and the refractive index of the surrounding medium. The refractive index of the surrounding medium will be affected both by changes in the chamber gas density and changes in the fuel vapor concentrations around the spray.

3.3. Discussion

This backscatter technique generates signals that are disturbed less by background problems because it selects light scattered from a specific depth, based upon the width of the time-gate and the delay between imaging and gating pulses. Furthermore, beam steering effects evident in the non-TG images are suppressed in the TG-sampled data. A plausible explanation for this effect is the preferential selection of light propagating a specific path length which suppresses the contributions from light propagating across the whole experimental volume. As a consequence the TG-sampled light will have traveled a shorter distance through the refractive index gradients
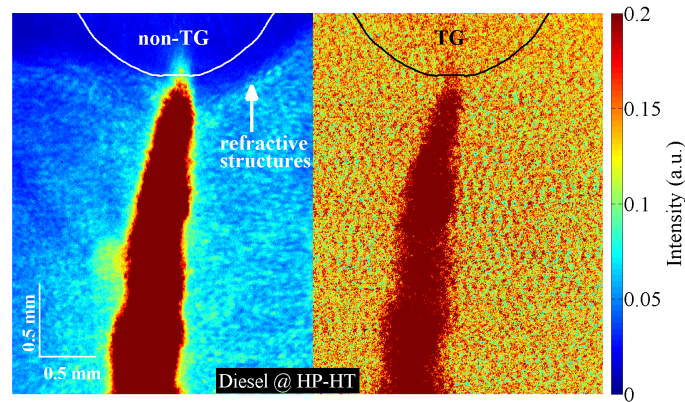
Fig. 7. TG and non-TG image of Diesel HP-HT shown in false color. The intensity has been normalized between 0 and 1 in each image. In the images a nozzle-tip outline has been added to help interpretation. Contrast adjusted to make the gas phase refractive structures in the non-TG image more visible.

of the medium and therefore the associated refractive effects are less apparent than in the non-TG case. Much like optical sectioning, the technique can also be used to probe depth by varying the TD.

Future improvements to the technique will involve using more energy in both gate and image pulses to improve the dynamic range in the TG images, to use an imaging setup with higher magnification for increased resolution, and to harmonize the depth of field and magnification with the size of the liquid structures under investigation. Depth of field can be adjusted somewhat by careful tuning of the OKE-gate length.
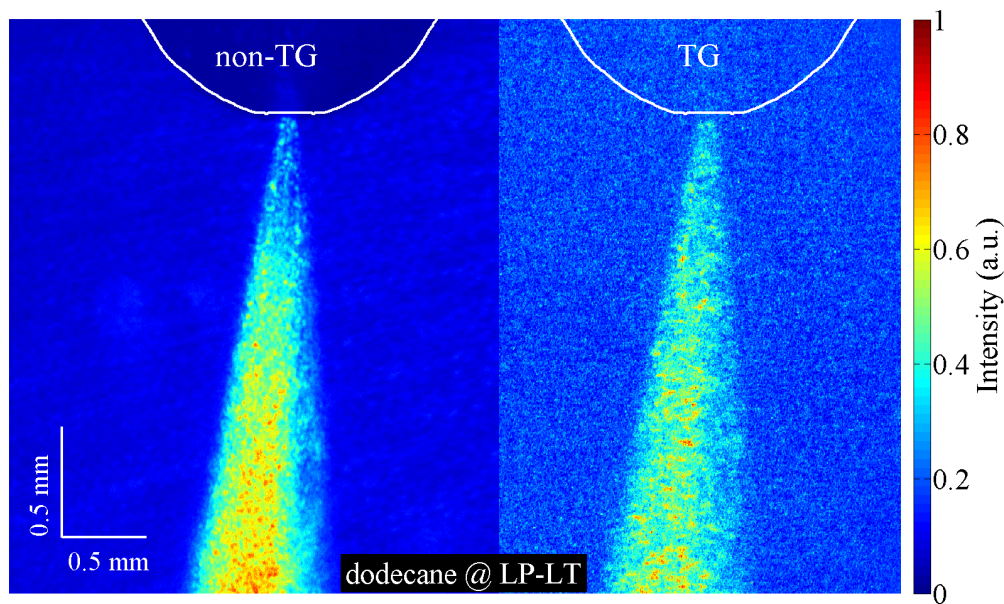
Fig. 8. TG and non-TG image of dodecane LP-LT shown in false color. The intensity has been normalized between 0 and 1 in each image. In the images a nozzle-tip outline has been added to help interpretation. For dodecane in the LP-LT condition reflections from larger fluid structures near the nozzle are less apparent than for Diesel in the same condition. A complete TG-scan from the dodecane LP-LT is provided as a video in Visualization 4.
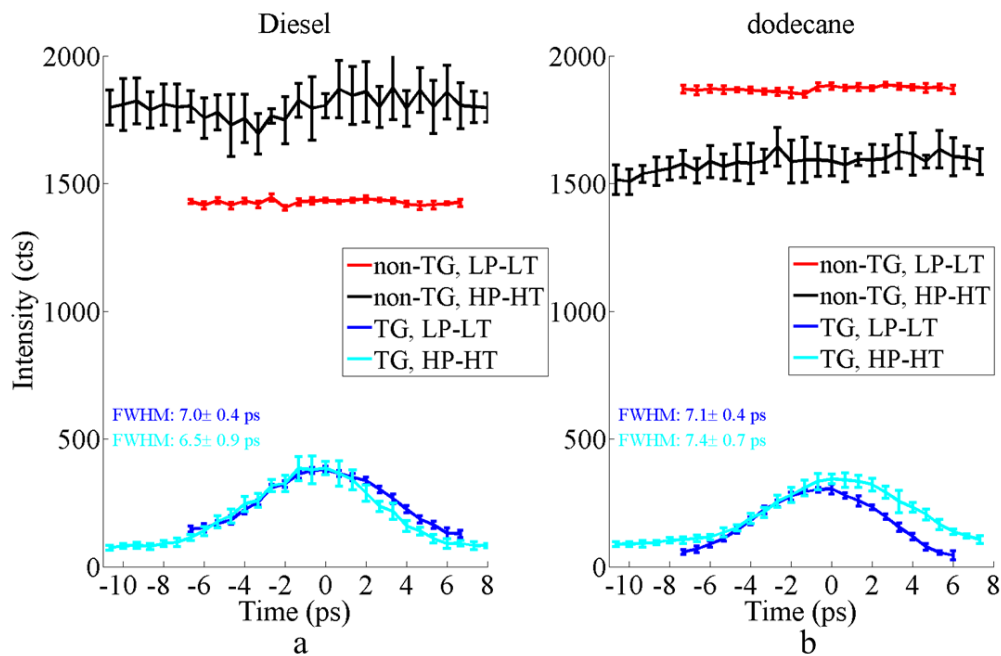

Fig. 9. Signals from TG and non-TG scans in the LP-LT and HP-HT conditions. Part a shows the Diesel case, and part b shows the dodecane case.

4. Conclusion

The time-gated backscattering approach based on the OKE-gate has demonstrated that depth within a spray can be spatially resolved by differences in the propagated path length of the scattered/reflected light. Using a CS_2 based OKE gate in a single-color, crossed-beam geometry generates a depth resolution around 0.45 mm. The contrast of reflections from larger fluid structures in the spray formation region are enhanced with the use of the time-gate, owing to the suppression of multiple scattering from the surrounding drops. The results presented here further indicate that beam steering effects due to refractive index gradients in and around the probed volume are suppressed in the time-gated images.

This technique holds promise for suppression of multiple-scattering, and it can provide backscattering imaging with depth resolution that is high enough for optical sectioning of the spray formation region in these industrially relevant sprays.

Acknowledgments